

**GT2011-4588\$**

## **A COMPARISON OF ADVANCED NUMERICAL TECHNIQUES TO MODEL TRANSIENT FLOW IN TURBOMACHINERY BLADE ROWS**

**Stuart Connell**

General Electric Global Research  
Niskayuna, NY, USA

**Mark Braaten**

General Electric Global Research  
Niskayuna, NY, USA

**Laith Zori**

ANSYS Inc  
Lebanon, NH, USA

**Robin Steed and Brad Hutchinson**

ANSYS Inc  
Waterloo, ON, Canada

**Graham Cox**

PCA Engineers  
Lincoln, England

### **ABSTRACT**

Computational predictions of the transient flow in multiple blade row turbomachinery configurations are considered. For cases with unequal numbers of blades/vanes in adjacent rows ("unequal pitch") a computation over multiple passages is required to ensure that simple periodic boundary conditions can be applied. For typical geometries, a time accurate solution requires computation over a significant portion of the wheel.

A number of methods are now available that address the issue of unequal pitch while significantly reducing the required computation time. Considered here are a family of related methods ("Transformation Methods") which transform the equations, the solution or the boundary conditions in a manner that appropriately recognizes the periodicity of the flow, yet do not require solution of all or a large number of the blades in a given row. This paper will concentrate on comparing and contrasting these numerical treatments.

The first method, known as "Profile Transformation", overcomes the unequal pitch problem by simply scaling the flow profile that is communicated between neighboring blade rows, yet maintains the correct blade geometry and pitch ratio. The next method, known as the "Fourier Transformation" method applies phase shifted boundary conditions. To avoid storing the time history on the periodic boundary, a Fourier series method is used to store information at the blade passing frequency (BPF) and its harmonics. In the final method, a pitch-wise time transformation is performed that ensures that the boundary is truly periodic in the transformed space. This method is referred to as "Time Transformation".

The three methods have recently been added to a commercially-available CFD solver which is pressure based and implicit in formulation. The results are compared and contrasted on two turbine cases of engineering significance: a high pressure power turbine stage and a low pressure aircraft engine turbine stage. The relative convergence rates and solution times are examined together with the effect of non blade passing frequencies in the flow field. Transient solution times are compared with more conventional steady stage analyses, and in addition detailed flow physics such as boundary layer transition location are examined and reported.

### **INTRODUCTION**

Some drivers relating to improving turbines are cost, performance and durability. Machine costs can be reduced if less components are used, however fewer components mean higher stage loadings, and more challenge for the aerodynamicist, if efficiency and range of operation are to be maintained. For aircraft engines, fewer components means less weight, which is a desirable outcome but this must be balanced against performance considerations that affect fuel burn and hence carbon emissions. High performance also requires maintaining or increasing turbine entry temperature, and the effect of these temperatures must be understood and designed for to maintain or improve durability. All of these drivers place demands on the design engineers, who rely on a combination of experience, test and analytical methods to meet these challenges. Virtual simulation plays an increasing role in the development process.

3D CFD simulation of turbine blade rows is central to the aerodynamic development of advanced turbines. With

the advancement in computational methods, models and flow solvers and the general availability of powerful computing facilities, blade row simulation has evolved from steady single passage simulation, to steady multiple blade row simulation to unsteady single and multiple blade row simulation.

Steady single blade row solution is now very fast, but information on adjacent rows must be specified, and the ability for adjacent rows to interact is only explicit at best. Steady multiple blade row methods such as the “mixing plane” approach and its variants extend simulation realism by including adjacent blade row effects, albeit in a limited manner. The limitation is due to the circumferential averaging and the manner in which information is communicated across the interface from one row to the next. The meridional effects of loss and blockage are therefore maintained, even though circumferential effects are “averaged out”. Despite such limitations, multi-blade row “stage” or “mixing-plane” methods represent a reasonable compromise between accuracy and efficiency and hence remain valuable and powerful tools for the designer/analyst.

In the context of turbine design, there are many reasons to perform transient analyses. The first of course is that the real flow is transient. It is of interest to determine the additional effects that are captured by a transient analysis and to what extent a transient analysis is justified as compared with a less expensive steady state simulation. Since turbines are already very efficient, it seems that further improvement to efficiency and durability requires a better understanding of observed physical phenomena such as wake propagation, wake-blade interaction, convection of hot streaks, transient loading variation, laminar-turbulent transition, complex endwall flows and primary-leakage flow interactions. The designer may wish to use a variety of tactics to improve the design, such as changing the loading distribution, blade “clocking”, adjusting sweep and lean or endwall contouring. The effect of each adjustment must be understood in the context of how it interacts with the unsteady flow, or not.

In the following, several transient, transformation based CFD flow methods are applied and evaluated as to their efficiency and effectiveness in evaluating transient flow phenomena on two turbine cases. The transformations performed are based on the primary unsteady frequency, the blade passing frequency. The effect of the transformation procedure on non blade passing frequencies is also considered and demonstrated for vortex shedding from a circular cylinder.

## NOMENCLATURE

BPF	Blade Passing Frequency
FT	Fourier Transformation
H	Total enthalpy
HPT	High Pressure Turbine

k	Turbulent kinetic energy
LPT	Low Pressure Turbine
PT	Profile Transformation
SST	Shear Stress Transport turbulence model
TRS	Transient Rotor Stator
TT	Time Transformation
U	Rotational velocity
$\Gamma$	Intermittency of turbulence
$\varepsilon$	Dissipation of turbulent kinetic energy
$\Theta$	Momentum thickness

Monitor point locations

LE	Leading edge
MPLE	Mid passage LE
MPTE	Mid passage TE
PSBL	Pressure surface boundary layer
SSBL	Suction surface boundary layer
TE	Trailing edge

## 1.0 TRANSFORMATION METHODS

The focus of this paper is transient CFD methods; however steady calculations are also performed and computing times reported for comparison purposes. The steady calculations use a mixing plane type of approach called a “stage interface”. Momentum and energy are conserved across the interface, but entropy increases as a result of the circumferential averaging process. All calculations are performed with a pre-release version of ANSYS CFX R13.0.

Transient calculations are performed using a recently-developed family of transient blade row methods known as “transformation methods”, namely Profile Transformation, Time Transformation and Fourier Transformation. These methods overcome the issue of unequal pitch in adjacent blade rows by transforming some quantity according to the specific method. These methods are compared to each other and to full/part-wheel calculations where periodic conditions apply. A brief description is provided below.

In Transient Rotor-Stator (TRS) simulations the true change in relative position of the rotor and stator are accounted for in fully implicit interface discretization. In these simulations, either full wheel is assumed or the smallest possible circumferential sector with an integer number of blades, according to the pitch ratio, is modeled with standard periodicity applied to the blade ensemble (unity ensemble pitch ratio between rotor and stator rows). We refer to this type of simulation as “full domain modeling” or “reference solution”.

In the Profile Transformation (PT) method (ANSYS, [1] also Galpin et al., [3]) a scaling procedure is applied automatically to solution profiles as part of the TRS implementation, whenever the rotor-stator pitch ratio is not unity. In this approximate method, single blade passages per row with different pitch lengths can be modeled without the need to geometrically scale or modify the blade geometry. Regular periodicity is imposed for each passage and flow profiles across rotor/stator

interfaces are automatically stretched or compressed as needed according to the pitch ratio while maintaining full conservation. Multiple passages can be used to reduce pitch scaling errors for the ensemble. Since this implementation is fully implicit and conservative a fast and robust transient solution can be obtained at a fraction of the time for a full domain model. While in this method overall machine performance is usually predicted well, detailed flow features such as blade passing signals will be inaccurate due to imposing instantaneous periodicity on the phase-shifted boundaries.

The Time Transformation (TT) method is based on the time-inclining work of Giles [5] but implemented on the Navier-Stokes equations in a fully implicit manner. This method can be considered as a correction to the Profile Transformation method in that the flow equations are transformed in time to ensure that the pitchwise boundaries are truly periodic (Biesinger et al., [2]). Therefore, the Time Transformation method maintains the robustness of the solution and also accounts for the correct blade passing signals between the rotor and stator. In the current implementation time transformation is also applied to the turbulent flow equations such as the  $k-\varepsilon$  and  $k-\omega$  family of turbulence models. While this method is fast and robust it suffers from two issues. First it is not extendable to multi-disturbance problems such as flow in a multi-stage configuration. Second, the transformation in time puts a physical constraint on the range of possible stage pitch ratios per rotor wheel speed, beyond which numerical instabilities will be encountered (Giles [5]).

The Fourier Transformation (FT) method is based on the fundamental work of He [6] and Gerolymos [4]. In this method the flow history on the phase-shifted pitchwise boundaries are stored using Fourier series at the blade passing frequency and its higher harmonics. At the rotor-stator interface flow information is stored using double-Fourier series by decomposing the solution history in time and azimuthal direction. The solution is then reconstructed on each side of the interface using Fourier coefficients from the opposite side. This strategy provides an excellent data compression by taking advantage of the periodic nature of the flow in the azimuthal direction. The one main difference between the current implementation and other published work (He [6], Gerolymos [4]) is the use of a double-passage strategy for collecting high quality signals between the two passages and using them on both sides of the pitchwise periodic boundaries with appropriate phase-shift (Biesinger et al [2]). But due to the explicit nature of the phase-shifted boundary condition the FT solution method will require more blade passing cycles for convergence than the TT method. However, unlike the TT method, the FT method is applicable for all rotor speeds and to very large pitch ratios. Most importantly this method can be extended to handle multi-

disturbance problems and thus multi-stage turbomachinery configurations.

## 2.0 HIGH PRESSURE TURBINE

The objectives of this evaluation are twofold: (i) to ensure that the transformation methods generate comparable solutions to the equivalent periodic case and (ii) to compare the computer time and memory requirements of the methods.

This test case is a rotor typical of a modern gas turbine, with inlet and exit relative Mach numbers of approximately 0.5 and 0.6 respectively. The peak suction surface relative Mach number is 1.0. A multi-block hexahedral mesh containing 720,000 nodes was generated for this case, with a near wall spacing suitable for a wall function calculation. This mesh is illustrated in Figures 1 and 2.

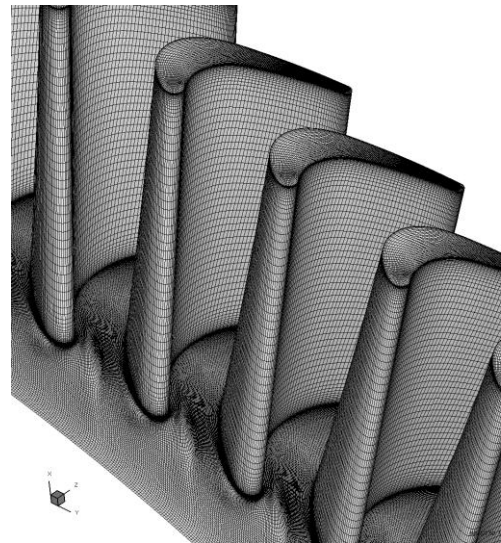


Figure 1 HPT rotor mesh.

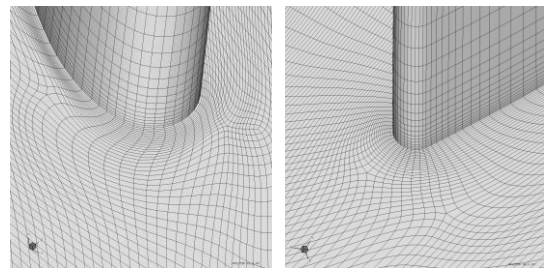
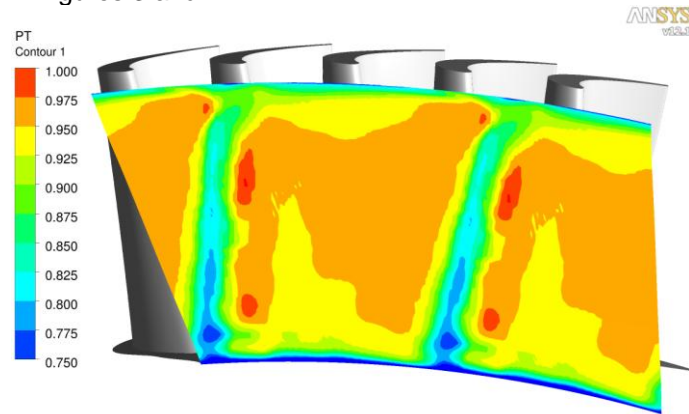


Figure 2 Leading and trailing edge mesh details for the HPT.

To evaluate the various transformation methods, the interaction of this rotor with its adjacent upstream stator is analyzed. To simplify the problem the effect of the upstream stator is modeled using a "frozen gust" representing the wake. This frozen gust is stationary in the absolute frame but rotates across the inlet of the rotor

when viewed in the relative frame. This gust was obtained from a steady state calculation on the stator, which included cooling flows in the model. This gust is illustrated in Figures 3 and 4.



**Figure 3 Absolute Total pressure at rotor inlet**

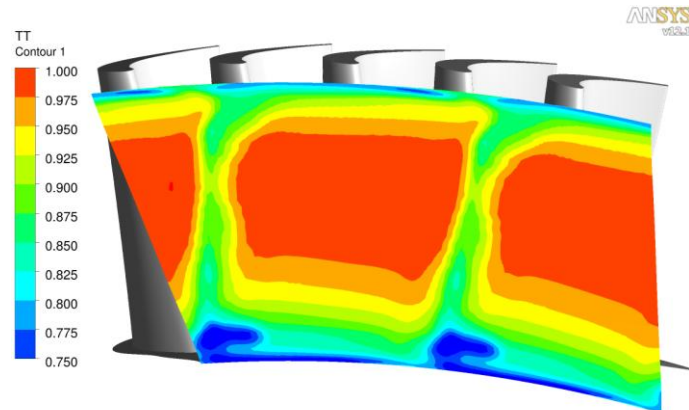


**Figure 1 Absolute total temperature at rotor inlet**

As designed the turbine stage has 92 rotors and 36 stators. For periodicity, a calculation of 23 rotor passages (one quarter wheel) would be required. To make the comparison more tractable the rotor count was adjusted slightly from 92 to 90, and so a periodic solution now requires a calculation of only five rotor passages.

In order to compare the solutions and to assess convergence to a periodic steady state a number of monitor points were inserted into the flow. The monitor point names and locations are described in the nomenclature.

An initial baseline unsteady run was made using a five passage grid and simple periodic boundary conditions. Subsequent equivalent runs were made using the FT and TT methods using two passages. All runs used fifty time steps per passing period. The FT method used ten Fourier modes. Calculations were performed using a pre-release version of ANSYS CFX R13.0. The primary modeling parameters were 2<sup>nd</sup> order discretization and k-ε turbulence model.

## 2.1 Results

Contours of total temperature at 50% span are compared in Figure 5. A comparison of the temporal variation in absolute total pressure at the monitor point locations is shown in Figure 6. All other variables showed a similar level of agreement. Ten modes were used for the FT calculations in all cases.

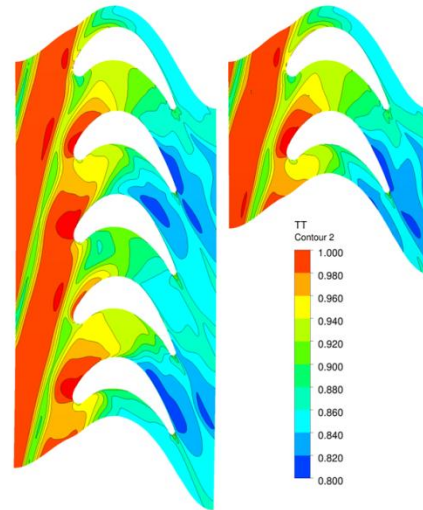


**Figure 2 Comparison of total temperature between Periodic (left) and FT (right) methods**

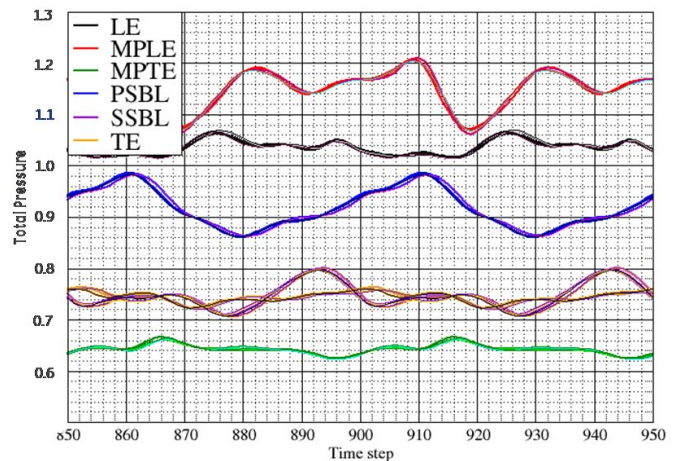


**Figure 6 Time varying total pressure plotted at six monitor points over two periods for the three methods: periodic (reference solution), FT and TT.**

The agreement between the periodic and transformed solutions is very good. The small discrepancies in the FT method are probably due to non blade passing frequency (BPF) modes modeled in the periodic solution but which are filtered in the FT solution. In section 4.0 the effect of non-BPF modes is investigated in more detail. The discrepancies in the TT method may relate to the lack of

time transformation of the viscous terms in the governing equations.

To assess the relative convergence rates of the methods to a periodic steady state the running average of a solution variable at the monitor points over a period was computed and compared to the same average from a well converged periodic steady state solution after 1000 time steps (twenty periods). The results of this convergence measure are shown in Figure 7. If convergence is defined as a 0.1% change then the five passage periodic case converges in approximately four periods. The TT method converges at an almost identical rate. The FT method takes approximately twelve periods to reach the same level of convergence. This test case is relatively simple with straight end-walls and no cavities. These fast convergence rates may deteriorate somewhat if additional flow features are included.

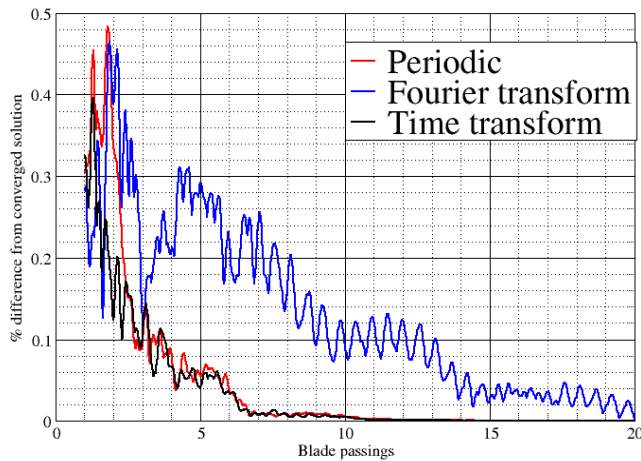


**Figure 7 Convergence rate of periodic and transformation methods.**

The change in convergence rates relates to the method in which the periodic phase shifted boundary condition is applied. With the periodic and TT methods the periodic boundary condition is fully implicit, matching the solver scheme and resulting in very similar convergence rates. In contrast the FT method employs an explicit treatment which slows the overall convergence rate.

The computing requirements of the methods will now be compared. Defining a computing unit as the CPU time required to perform one period (fifty time steps) on one passage provides a convenient way of comparing the methods. Table 1 compares the computing units required by the various methods to reach a converged solution. The time required for the correct geometry of 1/4 wheel or 23 passages for a periodic case is also included.

**Table 1 Comparison of computing time for HPT**

Method	passages required	# periods to convergence	# computing units
Periodic	5	4	20
Periodic	23	4	92
FT	2	12	24
TT	2	4	8

These results clearly demonstrate the efficiency of the transformation methods when compared to a multi-passage baseline periodic solution. The TT method achieves a reduction in computing units in excess of 10X over the 23 passage periodic case. The reduction for the FT method is less dramatic but still significant at almost 4X.

It can be estimated that the FT and periodic methods become equivalent for a periodic case that would require approximately six passages. It should also be noted that the large multi-passage cases will require significant computing resources in terms of memory and processing units compared to the two transformation methods.

### 3.0 LOW PRESSURE TURBINE

The low pressure turbine stage studied here was designed by PCA Engineers Ltd. for ANSYS, Inc., for numerical analysis purposes (it is not connected with any GE design). It is highly loaded, of the type sometimes used in the low pressure section of an aircraft engine. The blading is characterized by its thin cross section and relatively high aerodynamic loading and lift coefficient (Zweifel). Mechanical stresses in the blades could be expected to be higher than for more conventional blading,

**Table 2 LPT Stage design information**

# of stator blades	88
# of rotor blades	76
Rotational speed	3000 RPM
Work coefficient $[\Delta H/(U \cdot U)]$ (nominal)	2.8
Rotor Zweifel coefficient	1.35
Rotor RMS radius (at trailing edge)	0.643m
Stator inlet Mach number	0.36
Rotor inlet Mach number (relative)	0.45
Reynolds number (nominal)	1.0E5
Inlet turbulence intensity	4%

but this is a tradeoff against lower turbine mass. The casing is flared and the rotor blades shrouded, hence no tip gaps. Leakage flows are not included in the simulation. The geometry is displayed in Figure 8 and details are provided in Table 2.



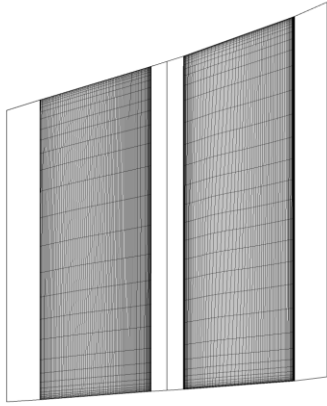


**Figure 8 Meridional view of the computational domain and blade surface mesh for the LPT.**

Solutions, both steady and transient, were obtained on several hexahedral grids, as reported in Table 3. All grids were generated using ANSYS TurboGrid. Table 3 lists the number of nodes for the stage consisting of one stator and one rotor passage. Nodes were divided approximately equally between the stator and the rotor. A portion of the medium grid is displayed in Figure 9. Calculations were performed using a pre-release version of ANSYS CFX R13.0, with second order spatial and temporal discretization. The flow was modeled as either fully turbulent, using the SST turbulence model of Menter [7], or as transitional, in which case the SST turbulence model is supplemented by the  $\Gamma$ - $\Theta$  transition model of Menter et al. [8].

**Table 3 LPT stage grid information (one stator and one rotor passage)**

Grid size	Total Nodes (stator + rotor)	Nodes in span	Average Blade $Y^+$
Coarse	478,000	39	0.17
Medium	1,183,000	51	0.17
Fine	2,288,000	82	0.17

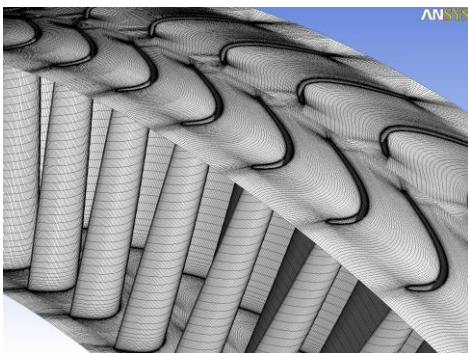


**Figure 9 LPT (medium) grid.**

### 3.1 Steady simulations

Steady simulations were performed to provide a starting point for the transient simulations. The steady solutions also provided information as to the change in the flow with grid refinement. Finally, it is interesting to compare the steady computing times to those of the various transient simulations, so the reader can obtain a more complete picture of the relative cost of simulation of the various methods. All steady simulations were performed with the “stage model”, which performs circumferential averaging at the stage interface.

It was observed that the “steady” simulations were only approximately so. This is due to observed small separated flow regions centered near mid-chord and extending from hub to shroud on the pressure side of both the rotor and the stator. This was expected, and is inherent to this particular type of LPT design.

### 3.2 Transient simulations

Transient simulations were performed on the medium grid, with the exception of the TT method, where a grid refinement study was performed and solutions obtained on all three grids. Results are summarized in Table 4, where the values listed were obtained by time-averaging over the final transient cycle. In the table, the simulation results are denoted by the method (“PT”, “TT”, “FT” or “1/4”, where “1/4” indicated the periodic reference solution) followed by the grid size (“C”=coarse, “M”=medium, “F”=fine). All medium grid (denoted by “M”

**Table 4 LPT stage steady and transient simulation results, relative to reference solution.**

Method -Grid	Relative Work Coefficient ( $\Delta H/U^*U$ )		Relative Stage Efficiency (isentropic)	
	without transition	with transition	without transition	with transition
PT-M	-0.03	0.00	-0.8	0.2
TT-C	-0.03	-0.02	-2.0	-1.1
TT-M	-0.03	0.00	-1.3	-0.2
TT-F	-0.04	-0.01	-1.6	-0.7
1/4 -M	-0.02	0.00	-1.0	0.0

in Table 4) simulations used the same number of nodes per passage (1,183,000, as per Table 3). However, the total number of nodes for the FT method is twice this, due to its “dual passage” formulation. The quarter-wheel reference case consists of 22 stators and 19 rotors, with 23,932,000 nodes in total.

Both fully turbulent predictions and those including the effects of laminar-turbulence transition are reported. Reported results are relative to the quarter-wheel with transition reference solution. Work coefficients for the transition cases are all close to the reference solution,

and are nearly identical for the medium grid cases. Concerning efficiency, the PT is within 0.2 points of efficiency of the reference solution, as is the TT method, except in the opposite direction. This is despite the approximation related to pitch scaling of the PT method. Compared with the transition solutions, the fully turbulent work coefficients are about 0.01 to 0.03 lower, and predicted efficiency is about one percentage point lower. The fully turbulent transformation solutions relate to their corresponding reference solution in much the same way as do the transitional cases.

Computational effort comparisons are provided in Table 5. All reported results are for the medium grid density. “# of Rotor Passes” is the number of times the rotor grid must pass the corresponding stator sector to obtain repeating results. “# of Coeff. Updates” indicates the number of times matrix coefficients are updated per time step, in order to provide time accurate results. Grid size is scaled relative to that used for the steady analysis. All calculations used 60 time steps per rotor pass, except for the FT solutions, which used 66. Relative computing effort is scaled to that required by the steady method. Results indicate that transient solutions obtained using the transformation methods required approximately 20 to 65 times the CPU effort required by a steady analysis. However, computing effort is approximately an order of magnitude smaller than that required for the quarter-wheel reference solution.

**Table 5 LPT stage computational effort**

Method-Grid	# of Rotor Passes	# of Coeff. Updates	Relative Grid Size	Relative Effort
ST-M	1.5	1	1	1.0
PT-M	11	3	1	22.0
TT-M	11	5	1	36.7
FT-M	16	3	2	64.0
¼ -M	11	3	20	440.0

Figure 10 compares the predicted time-averaged mid-span Mach number for the TT, PT and reference cases, (no transition). Close examination indicates an almost identical flow pattern. Figure 11 compares time and meridional-averaged Mach number for the TT and reference solutions. Again, these averaged flow patterns are very similar.

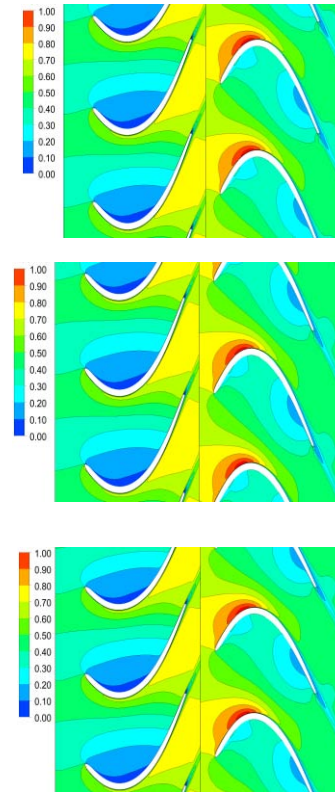


Figure 10 LPT: Comparison of time-averaged mid-span Mach number for TT (top), PT (middle) and the reference case (bottom) [no transition].

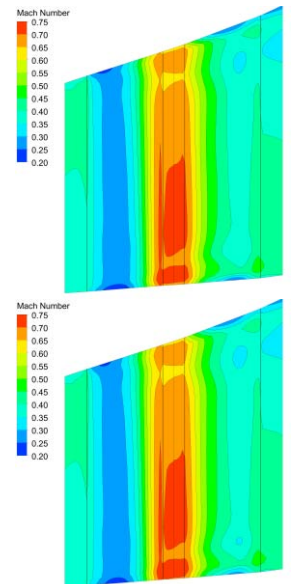
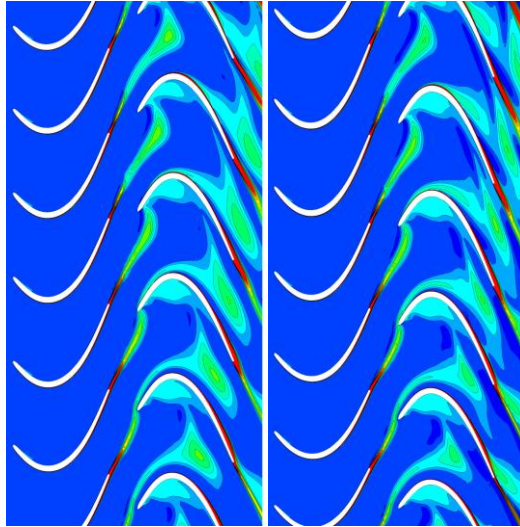


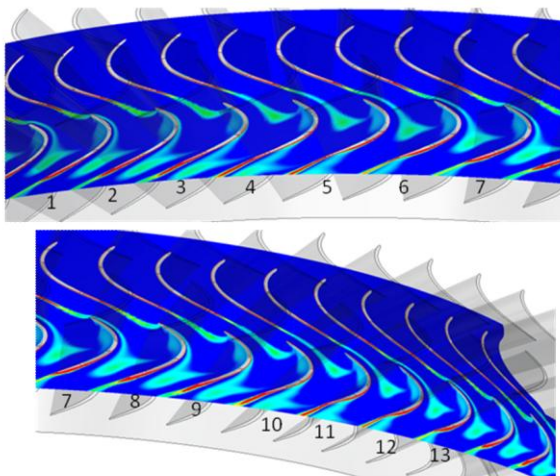
Figure 11 LPT: Comparison of time and meridional-averaged Mach number for the TT (top) and reference (bottom) solutions, with transition on.

Figure 12 compares instantaneous predictions of entropy at mid-span for the reference solution and the TT solution. While there are small differences in levels, predicted flow patterns are very similar. The transient interaction of the stator wake with the rotor can be observed by looking at the left sequence, from bottom to top. The stator wake enters the rotor passage and grows both laterally and in the streamwise direction. This process continues as the stator wake is “chopped” by the leading edge of the rotor blade and convects downstream. The rotor also exhibits a comparatively stable region of high entropy, near mid-chord on the pressure side, which corresponds to a region of recirculating flow.



**Figure 12 LPT: Comparison of instantaneous entropy at mid-span, for the reference solution (left) and the TT method (right), with transition on.**

Figure 13 is similar to Figure 12 in that mid-span entropy is again displayed, although over a larger number of blades. The sequence of blades has been split, with rotor passages 1 through 7 shown in the upper part of the figure. Passage 7 also appears in the lower part of the figure, along with passages 8 through 13. The stator wake is cut at a frequency of just slightly less than every 6 rotor blade passes, as can be seen by viewing the rotor leading edge on the left side of passages 1, 7 and 13. The initial development of the stator wake in the rotor passage can be seen by looking at the right side (pressure side) of passage 1. One can also see the development of the new wake just after it has been cut by the rotor leading edge.



**Figure 13 LPT: Entropy at midspan (transition on).**

The wake slowly migrates towards the suction side of the passage, while convecting downstream. By passage 6 the wake has convected to about 60% rotor axial chord. In passage 7 the “tail” of the wake is cut by the leading edge of the rotor. The tail of the wake (see passage 8, left side, leading edge) convects along the suction side of the blade (see passages 8 through 12) and finally exits the rotor passage, as seen in passage 13. The pattern is similar for passages 2 through 6. At the rotor trailing edge, passage 5 through 8 show that the rotor wake is comprised of the coalescence of the convected stator wake with the rotor boundary layer. The convection of the stator wake through the rotor boundary layer is observed to affect the location of the suction side transition location, since the transition model is based on local flow conditions.

The preceding description is relative to the mid-span flow. Figure 14 provides a view at axial locations corresponding to rotor mid-chord (upper) and rotor exit (lower). At mid-chord, passages 2 through 8 display the migration process. In passages 2 and 3 the stator wake appears, in 4 and 5 the bulk of the wake passes, in 6 and 7 the tail of the wake is close to the suction surface and in passage 8 the old wake has passed and a new wake is just starting to appear (at the hub). The figure also shows the spanwise variation in wake strength, which is strongest near the shroud, followed by the near hub region.

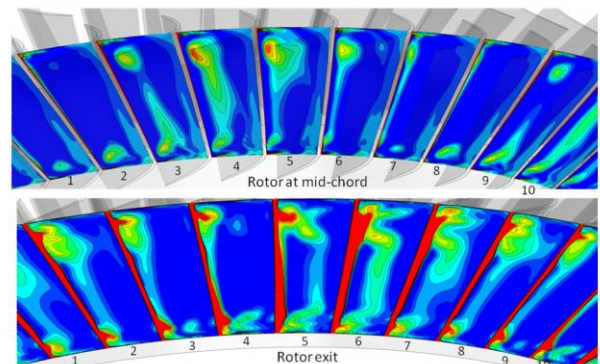


**Figure 14 LPT: Entropy at rotor mid-chord (upper) and at rotor exit (lower) (transition on), looking upstream.**

The lower part of Figure 14 shows conditions at the rotor exit. The bright red indicates the entropy generated by the blade boundary layers, and the increased entropy levels near hub and shroud associated with the stator wakes are clearly visible. The suction (left) side of passages 4 and 10 indicate relatively clean flow since the stator wake has passed, while passages 5 through 9 indicate the progressive convection of the stator wake and its



eventual migration towards the suction side of the blade passage (see passage 9).

#### 4.0 EFFECT OF TRANSFORMATION METHODS ON NON-BPF FREQUENCIES

The FT and TT methods are intended to model cases which contain a dominant frequency (blade passing) and its harmonics. It is interesting to investigate how these methods perform on a case that does not satisfy this criterion. An example would be a self-excited phenomenon such as trailing edge vortex shedding. To assess the effect of the FT and TT methods on such cases the vortex shedding from a circular cylinder was considered. The geometry was designed so that the vortex street passes through the periodic boundary. The two passage geometry used in this case is illustrated in Figure 15. For the solution parameters chosen the shedding frequency was found to be 500Hz. Figure 16 shows the calculated vortex street passing through the lower periodic boundary.

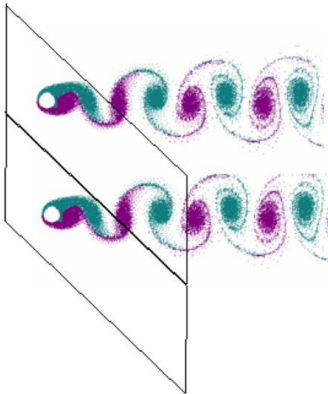


Figure 15 Vortex shedding model problem.

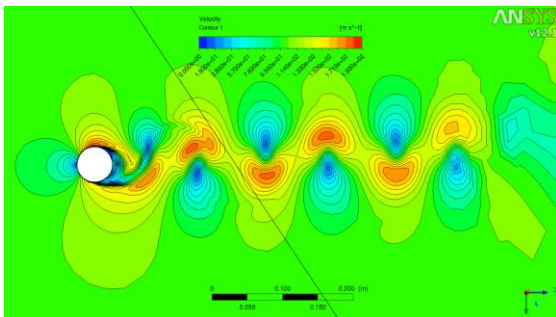


Figure 16 Vortex shedding through a periodic boundary with a shedding frequency of 500Hz .

The upper and lower periodic boundaries shown in Figure 15 were now replaced with time shifted boundaries employing the FT or TT methodology with a BPF equal to the shedding frequency. Figure 17 shows the result of this calculation for the FT method on the lower periodic boundary. To illustrate how the vortex street passes

through this boundary a copy of the upper passage is displayed next to the lower passage. It will be noted that the vortex street passes cleanly through the FT boundary. The phase shift at the boundary results from the display method described above. The TT method showed similar results.

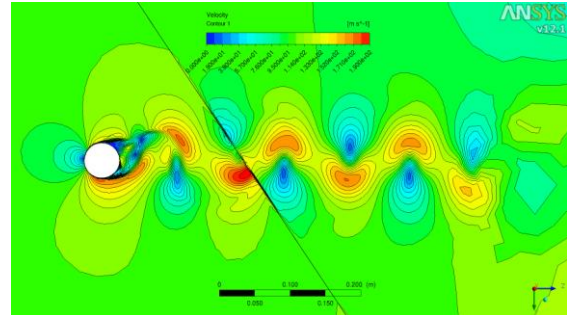


Figure 17 Vortex shedding through FT boundary with BPF = shedding frequency of 500Hz

In the next case the blade passing frequency was adjusted to 400Hz, this ensured that neither the BPF or any harmonics matched the shedding frequency. The results are shown in Figure 18 for the FT method and Figure 19 for the TT method. In this case it will be observed that the vortex street is highly damped as it passes through the FT boundary. This is due to the filtering effect of the boundary condition that only permits BPF and harmonics to cross the periodic boundary. In contrast the TT method shows no damping.

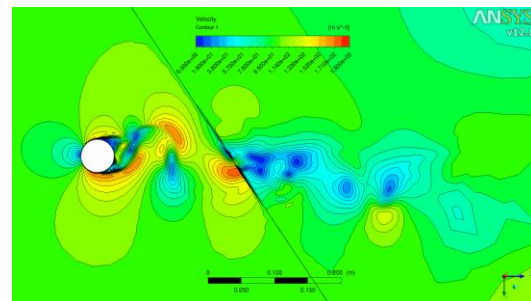


Figure 18 Vortex shedding through a FT boundary with a BPF=400Hz.

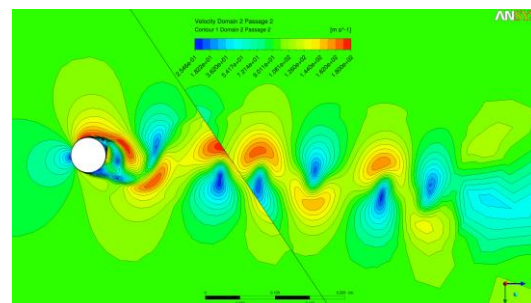


Figure 19 Vortex shedding through a TT boundary with a BPF=400Hz.

## CONCLUSIONS

The three transformation methods, PT, FT and TT, have been evaluated and compared on a range of test cases. The exact choice of which method to employ for optimum use of computer resources and temporal accuracy depends on a number of parameters, including:

Type of solver algorithm employed: implicit/explicit

Relative blade counts

Frequency content of solution

Number of components to be solved

Considering each method in turn:

Periodic (no transformation)

- Requires full or part wheel calculations with associated memory and run time requirements
- Will capture all frequency content of solution

Profile Transformation

- Requires one or a small number of passages according to relative blade counts and accuracy desired.
- An option which allows the user to trade off speed with accuracy
- Converges at same rate as periodic method
- Applicable to multi-stage configurations
- Can be used in conjunction with other transformation methods

Time Transformation

- Requires (typically) only one passage resulting in reduced run time/memory for periodic cases that would require significant part of wheel (stability criterion will lead to the need for multiple passages in some cases).
- Converges at same rate as periodic method
- Non-BPF + harmonic modes are not damped
- Limited to a single stage

Fourier Transformation

- Requires two passages resulting in reduced run time/memory for periodic cases that would require all or a significant part of the wheel
- The FT periodic condition is treated in an explicit manner which tends to slow convergence of implicit methods. This effect will not be seen in explicit methods
- Will filter frequency components which are non-BPF + harmonics
- Applicable to multi-stage configurations and fluid-mechanical applications such as aerodynamic damping analysis

If we consider a stage calculation then the simple PT method will be stable and robust for all conditions at the expense of temporal accuracy. If the time accuracy of solutions is important then the other transformation methods (TT, FT) together with a periodic part wheel solution should be considered. The TT method will

perform well if the associated stability criterion is satisfied. If the TT method is not suitable then the FT method will perform well. However if the case under consideration only requires a few passages for periodicity then the periodic method may be a viable option.

For multistage solutions the PT method will again perform well at the expense of temporal accuracy. The current implementation of the time transformation method is not suitable for these applications due to the fixed transformation. FT methods can be employed for multistage calculations. Again if only a few passages are required for periodicity the periodic method may provide the best option.

## ACKNOWLEDGMENTS

The authors wish to acknowledge Mahesh Athavale of GE for his help in generating the mesh and gust boundary conditions for the HP turbine case and Philippe Godin and Rubens Campregher of ANSYS for their assistance with the CFD simulations.

## REFERENCES

- [1] ANSYS CFX Version 12 documentation, ANSYS Inc., 2009
- [2] Biesinger T., Cornelius C., Rube C., Schmid G, Braune A., Campregher C., Godin P., Zori L, 2010, "Unsteady CFD Methods in a Commercial Solver For Turbomachinery Applications", Proceedings of the ASME Turbo Expo 2010, GT2010-22762
- [3] Galpin P.F., Broberg R.B., Hutchinson B.R., "Three-Dimensional Navier Stokes Predictions of Steady State Rotor/Stator Interaction with Pitch Change", Third Annual Conference of the CFD Society of Canada, June 27-27, 1995, Banff, Alberta, Canada
- [4] Gerolymos G., Michon G., Neubauer J., 2002, "Analysis and Application of Chorochronic Periodicity in Turbomachinery Rotor/Stator Interaction Computations", Journal of Propulsion and power, Vol 9, no. 6, pp. 1139-1152
- [5] Giles, M., 1988, "Calculation of Unsteady Wake/Rotor Interaction", Journal of Propulsion and Power, 4(4), pp. 356-362
- [6] He, L., 1990, "An Euler Solution for Unsteady Flows Around Oscillating Blades", ASME Journal of Turbomachinery, 12, pp. 714-722
- [7] Menter, F.R., 1994, "Two-equation eddy-viscosity turbulence models for engineering applications", AIAA-Journal, 32, (8), pp. 1598 - 1605
- [8] Menter, F.R., Langtry, R.B., Likki, S.R., Suzen, Y.B., Huang, P.G., 2004, "A Correlation Based Turbulence Model Using Local Variables, Part 1 - Model Formulation", Proceedings of the ASME Turbo Expo 2004, GT2004-53452